



HAL
open science

Trade-offs in biodiversity and ecosystem services between edges and interiors in European forests

Thomas Vanneste, Leen Depauw, Emiel de Lombaerde, Camille Meeussen,
Sanne Govaert, Karen de Pauw, Pieter Sanceruk, Kurt Bollmann, Jörg Brunet,
Kim Calders, et al.

► To cite this version:

Thomas Vanneste, Leen Depauw, Emiel de Lombaerde, Camille Meeussen, Sanne Govaert, et al..
Trade-offs in biodiversity and ecosystem services between edges and interiors in European forests.
Nature Ecology & Evolution, 2024, 8, pp.880-887. 10.1038/s41559-024-02335-6 . hal-04486632

HAL Id: hal-04486632

<https://hal.science/hal-04486632v1>

Submitted on 31 Oct 2024

HAL is a multi-disciplinary open access archive for the deposit and dissemination of scientific research documents, whether they are published or not. The documents may come from teaching and research institutions in France or abroad, or from public or private research centers.

L'archive ouverte pluridisciplinaire **HAL**, est destinée au dépôt et à la diffusion de documents scientifiques de niveau recherche, publiés ou non, émanant des établissements d'enseignement et de recherche français ou étrangers, des laboratoires publics ou privés.

1 **Title**

2 Trade-offs in biodiversity and ecosystem services between edges and interiors in European forests

3 **Author list**

4 Thomas Vanneste^{1,*},§, Leen Depauw^{1,§}, Emiel De Lombaerde¹, Camille Meeussen¹, Sanne Govaert¹,
5 Karen De Pauw¹, Pieter Sanczuk¹, Kurt Bollmann², Jörg Brunet³, Kim Calders⁴, Sara A. O. Cousins⁵,
6 Martin Diekmann⁶, Cristina Gasperini⁷, Bente J. Graae⁸, Per-Ola Hedwall³, Giovanni Iacopetti⁷,
7 Jonathan Lenoir⁹, Sigrid Lindmo⁸, Anna Orczewska¹⁰, Quentin Ponette¹¹, Jan Plue⁵, Federico Selvi⁷,
8 Fabien Spicher⁹, Hans Verbeeck⁴, Florian Zellweger², Kris Verheyen¹, Pieter Vangansbeke¹ and Pieter
9 De Frenne¹

10 **Affiliations**

11 ¹ Forest & Nature Lab, Department of Environment, Faculty of Bioscience Engineering, Ghent
12 University, Geraardsbergsesteenweg 267, 9090 Melle-Gontrode, Belgium

13 ² Swiss Federal Institute for Forest, Snow and Landscape Research WSL, Zürcherstrasse 111, 8903
14 Birmensdorf, Switzerland

15 ³ Southern Swedish Forest Research Centre, Swedish University of Agricultural Sciences, Box 190, 234
16 22 Lomma, Sweden

17 ⁴ CAVElab – Computational and Applied Vegetation Ecology, Department of Environment, Faculty of
18 Bioscience Engineering, Ghent University, Coupure Links 653, 9000 Ghent, Belgium

19 ⁵ Biogeography and Geomatics, Department of Physical Geography, Stockholm University, Svante
20 Arrhenius väg 8, 106 91 Stockholm, Sweden

21 ⁶ Vegetation Ecology and Conservation Biology, Institute of Ecology, FB2, University of Bremen,
22 Leobener Str. 5, 28359 Bremen, Germany

23 ⁷ Department of Agriculture, Food, Environment and Forestry, University of Florence, P. le Cascine 28,
24 50144 Florence, Italy

25 ⁸ Department of Biology, Norwegian University of Science and Technology, Høgskoleringen 5, 7491
26 Trondheim, Norway

27 ⁹ UMR CNRS 7058 « Ecologie et Dynamique des Systèmes Anthropisés » (EDYSAN), Université de
28 Picardie Jules Verne, 1 Rue des Louvels, 80037 Amiens, France

29 ¹⁰ Institute of Biology, Biotechnology and Environmental Protection, Faculty of Natural Sciences,
30 University of Silesia, Bankowa 9, 40-007 Katowice, Poland

31 ¹¹ Earth and Life Institute, Université catholique de Louvain, Croix du Sud 2, 1348 Louvain-la-Neuve,
32 Belgium

33 * Corresponding author: thomas.vanneste@ugent.be

34 [§] These authors contributed equally

35 **Abstract**

36 Forest biodiversity and ecosystem services are hitherto predominantly quantified in forest interiors, well
37 away from edges. However, these edges also represent a significant proportion of the global forest
38 cover. We quantified plant biodiversity and ecosystem service indicators in 225 plots along forest edge-
39 to-interior transects across Europe. We found strong trade-offs: phylogenetic diversity (evolutionary
40 measure of biodiversity), proportion of forest specialists, nutrient cycling and heatwave buffering
41 increased towards the interior, whereas species richness, nectar production potential, stemwood biomass
42 and tree regeneration decreased. These trade-offs were mainly driven by edge-to-interior structural
43 differences. As fragmentation continues, recognizing the role of forest edges is crucial for integrating
44 biodiversity and ecosystem service considerations into sustainable forest management and policy.

45

46 **Main text**

47 Forests harbor the majority of terrestrial species on earth and provide a multitude of ecosystem services
48 to humans, including carbon sequestration, timber production, nutrient cycling, water cycling and
49 climate buffering¹. However, most forest biodiversity and ecosystem service assessments report data
50 from forest interiors, well away from edges and their complex influences on biodiversity (see e.g. ^{2,3}).
51 This is most often done intentionally, to avoid complex interactions and exclude the environmental
52 differences between forest edges and interiors including edges' warmer microclimates⁴, higher light
53 availability⁵ and enhanced soil nutrient inputs from adjacent land-use⁶. Ongoing forest fragmentation,
54 however, increases the relative amount of the area covered by forest edges and causes edge effects to
55 penetrate more frequently and deeply into the forest interior. Edge effects can potentially reach the core
56 in small forest fragments^{7,8}. Up to 70% of the world's remaining forest is now found within 1 km of a
57 forest edge and 20% is even closer than 100 m⁹. In fact, recent global inventories have shown that the
58 loss of forest interior area is at least twice as high as the net loss of forest area¹⁰. In Europe, the situation
59 is even more precarious with 40% of forests lying within 100 m of the edge¹¹. As fragmentation persists
60 globally, edges will play an increasingly important role in future forest functioning and service
61 provisioning, and can no longer be ignored in conservation decision-making, forest policies, and
62 management planning. In spite of the urgency, no continental-scale study to date has quantified edge
63 vs. interior patterns of the potential supply in terms of forest ecosystem services and biodiversity.

64 Here we quantified a broad range of biodiversity indicators and ecosystem services in 225 plots along
65 45 forest edge-to-interior transects across a 2300-km wide latitudinal gradient across Europe (**Extended**
66 **Data Figure 1, Table S1**). We specifically investigated outer forest edges (sensu ¹²), where forest
67 patches border on large non-forest areas (e.g. arable fields or grasslands). To quantify biodiversity, we
68 focused on understorey plants as they represent the majority of plant biodiversity in temperate forests
69 and play a crucial role for temperate forest functioning¹³. Understorey plants are directly linked to
70 several forest ecosystem services, for instance via their impact on water cycling¹⁴, nutrient dynamics¹⁵
71 and forest regeneration¹⁶, and may strongly shape forest ecosystem responses to global change^{17,18}.
72 Multiple facets of biodiversity were considered including taxonomic (total richness of species and

73 relative amount of forest specialists), phylogenetic (variety of evolutionary lineages) and functional
74 diversity (presence of different growth forms and resource use strategies) of the understorey plant
75 community because of their simultaneous but often contrasting influence on ecosystem service
76 provisioning¹⁹. In addition to these biodiversity attributes, we looked at several ecosystem services
77 covering a mixture of regulating (soil carbon storage, pollination potential, heatwave buffering and
78 decomposition) and provisioning services (timberwood, usable plants and tree regeneration). To
79 quantify the potential supply of these ecosystem services, different indicators were selected based on
80 an extensive literature search (see **Extended Data Figure 2** and *Methods* for more details). Using a
81 multivariate Bayesian modeling framework, specifically suited to study trade-offs, we then assessed
82 how the selected biodiversity and ecosystem service indicators changed with increasing distance to the
83 forest edge, while also accounting for gradients in latitude and forest management intensity (see
84 **Methods S1** for details on the model structure). Next, we evaluated the effects of several environmental
85 drivers on biodiversity and ecosystem service delivery potential, ranging from edaphic properties (soil
86 texture, soil acidity and leaf litter quality) over forest stand characteristics (forest structural complexity,
87 tree species composition and microclimate) to landscape-scale conditions (forest cover, drought and
88 nitrogen deposition).

89 We found complex trade-offs in biodiversity indices and ecosystem service delivery along forest edge-
90 to-interior transects across Europe. While phylogenetic diversity, proportion of forest specialists,
91 decomposition and heatwave buffering exhibited an increase towards the forest interior, other
92 biodiversity indices and ecosystem services such as taxonomic richness, pollination potential,
93 timberwood and tree regeneration were promoted towards the forest edge. However, functional
94 understorey plant diversity, soil carbon storage and the amount of usable plants remained unchanged
95 between the forest interior and the edge (**Figure 1**).

96 The trade-offs we found among ecosystem services also represent important trade-offs for management
97 and conservation assessments. Promoting landscapes with large, continuous forest cover or a few large
98 patches would maximize the delivery of some ecosystem services that prevail in forest interiors, at the
99 expense of other services that reach their highest level in forest edges. On the contrary, complex

100 heterogeneous landscapes with a mixture of both small and large forest patches, and thus a well-
101 balanced mixture of forest edge and interior area, are most likely to deliver, at least, moderate levels of
102 a broad array of ecosystem services. The latter echoes perfectly the principle of “*a jack of all trades is*
103 *a master of none, but oftentimes better than a master of one*” which was already introduced as a
104 mechanism underlying biodiversity-ecosystem multifunctionality relationships in forest interiors²⁰.
105 Here we show that, from a landscape point of view, the complementarity of edge and interior area is
106 also needed to ensure the simultaneous delivery of multiple ecosystem services in forests. Moreover,
107 an additional analysis using a multifunctionality index revealed that there was no pattern in multiservice
108 delivery from edge to core in the forest patches, confirming that trade-offs between ecosystem services
109 require stand-specific management strategies to optimize forests for specific or multiple ecosystem
110 services (**Extended Data Figure 3**).

111 Plant area index (PAI) is defined as the one-sided surface area of vegetation material per unit ground
112 surface area, and is a good proxy for forest structural complexity^{4,21}. We found that PAI was the
113 predominant driver of the observed trade-offs in biodiversity and ecosystem service delivery with
114 significant positive effects on phylogenetic and functional diversity, decomposition and microclimate
115 buffering but a negative effect on taxonomic richness. The effects of PAI show trends very similar to
116 the effects of the distance to the edge, suggesting that edge effects are mostly driven by forest structure
117 (**Figure 2**). Pollination potential was higher and heatwave buffering stronger when the canopy had a
118 higher shade-casting ability, whereas a warmer forest microclimate enhanced decomposition
119 (**Figure 2**). At the stand level, forest management practices that manipulate the structural complexity
120 of the canopy layer can thus play a key role in the local optimization of ecosystem services’ delivery.
121 Indeed, management actions that increase variability in canopy density and promote heterogeneity in
122 tree sizes and crown morphologies will result in a higher variety of resources and microhabitats thereby
123 promoting species coexistence and enhancing multiservice delivery²²⁻²⁵. The most important edaphic
124 condition was soil pH, having a positive effect on the proportion of forest specialists, taxonomic
125 richness and stemwood biomass. None of the landscape conditions had a strong effect on multiple
126 biodiversity indices or ecosystem services (**Extended Data Figure 4**).

127 Our results are relevant for forest management, nature conservation and environmental policy. We
128 recommend that future policies and strategy documents (e.g. the EU Biodiversity Strategy and Forest
129 Strategy) consider the importance of edges in maintaining and fostering the biodiversity and ecosystem
130 service delivery of European forests. At a landscape level, we show that both forest interiors as well as
131 forest edges, preferably with a contrasting structural complexity, are needed to guarantee the
132 simultaneous delivery of multiple ecosystem services rather than maximizing a few target services at
133 the expense of others. These trade-offs, however, depend on the stakeholder's priorities and require
134 tailored management practices. At the local scale, forest management practices can further determine
135 the delivery of specific ecosystem services (or a combination thereof) through canopy management
136 (e.g., opening vs. densification). Both forest edges and interiors fulfil an important role in our present-
137 day landscapes, and this should be taken into account when designing policy instruments and
138 management strategies that ensure their future conservation.

139 **Methods**

140 1. Study area and experimental set-up

141 Our study was conducted in broadleaved forests in nine regions spanning a ± 2300 -km wide latitudinal
142 gradient across the European sub-Mediterranean and temperate forest biomes (**Extended Data**
143 **Figure 1**). This latitudinal gradient covers a mean annual temperature (MAT) range of >10 °C, while
144 mean annual precipitation (MAP) varies between 550 and 1250 mm (long-term average values for 1979-
145 2013 retrieved from the CHELSA database²⁶). In each region, broadleaf forest stands larger than 4 ha
146 were selected with a dominance of oak species (chiefly) as these are important forest stands for
147 biodiversity in Europe²⁷. *Quercus robur*, *Q. petraea* and *Q. cerris* were the dominant species, but locally
148 complemented by *Alnus incana*, *Betula pubescens*, *Carpinus betulus*, *Fagus sylvatica*, *Populus tremula*
149 and *Ulmus glabra*. Specifically, three forest stands were selected per region with contrasting
150 management intensity: (1) 'dense forests' that were not thinned over the past 10-30 years, with a high
151 basal area (mean \pm SE was here 28.8 ± 1.5 m²/ha) and high canopy cover (openness $5.8 \pm 0.6\%$, mean
152 of three densiometer measurements), (2) 'medium dense forests' with frequent thinning and most recent

153 thinning about 5-10 years ago (basal area 31.4 ± 1.9 m²/ha, openness $6.5 \pm 0.6\%$) and (3) ‘open forests’
154 with the most recent thinning less than 4 years before sampling, with a low basal area (21.6 ± 1.3 m²/ha)
155 and low canopy cover (mean openness $14.8 \pm 2.1\%$). In three regions (Belgium, Central Italy and
156 Central Norway), forests of contrasting management intensity were selected at three elevation levels
157 (low, intermediate and high elevations range between 26-365 m in Belgium, 115-908 m in Italy and 21-
158 700 m a.s.l in Norway) to include an additional macroclimatic gradient caused by elevation of 1.5-4 °C
159 MAT. In the other six regions, only lowland forest stands were selected with elevations ranging between
160 7 and 451 m a.s.l. This added up to 45 forest stands in total (see **Extended Data Figure 1, Table S1**).

161 In each forest stand, a 100-m transect was then established perpendicular to the south-facing forest edge.
162 Five plots of 3 m × 3 m were installed along each transect, with their plot centers at an exponentially
163 increasing distance from the focal forest edge (1.5, 4.5, 12.5, 35.5 and 99.5 m). All plots were at least
164 100 m away from any forest edge other than the focal forest edge (**Extended Data Figure 1, Table S1**).
165 Vegetation surveys in these plots took place during the peak of the vegetation season (May-June 2018)
166 according to the local phenology. In each plot, all vascular plant species were identified and their
167 percentage ground cover was estimated relative to the plot area. Surveys were performed for every
168 forest stratum separately (herb layer = all vascular plant species below 1 m, including seedlings, shrubs
169 species and lianas, shrub layer = all shrub and tree species between 1-7 m and tree layer = all shrub and
170 tree species taller than 7 m). Furthermore, soil and litter samples were collected from each plot, the
171 forest structure was characterized using LiDAR and soil and air temperatures were measured using
172 microclimate loggers. More details on selection criteria and establishment of the plot network can be
173 found below as well as in ²⁸⁻³⁰.

174 2. Quantifying biodiversity and the potential supply of ecosystem services

175 2.1. Biodiversity

176 For each 3 m × 3 m plot, four biodiversity metrics were quantified for the understorey plant community,
177 i.e., taxonomic diversity, proportion of forest specialists, phylogenetic diversity and functional
178 diversity. Our focus on understorey biodiversity is justified because the understorey harboured on

179 average 77.6% of all vascular plant species per plot, while the shrub and tree layer contained only 10.2%
180 and 12.2% of all species, respectively. Taxonomic diversity was quantified as the total number of plant
181 species per plot in the forest understorey. The relative number of forest specialists in the understorey
182 was calculated based on the forest affinity categories defined in ³¹. All species categorized as 1.1 and
183 1.2 in this Europe-wide database of forest plant species were grouped as forest specialists (see ²⁸).
184 Phylogenetic diversity was quantified as the phylogenetic species variability (i.e. variation in
185 evolutionary history) of the herb community, and based on the molecular megaphylogeny of land plants
186 constructed by ³². Functional diversity was calculated as Rao's quadratic entropy based on relative
187 species abundances and pairwise functional differences among species³³. Three key functional traits
188 were selected following the leaf-height-seed scheme for plant ecological strategies, i.e., seed mass,
189 specific leaf area (SLA) and plant height. Trait values were standardized to mean zero and unit variance,
190 and subsequently used to compute a species-species Euclidean distance matrix with Cailliez correction
191 method to account for negative eigenvalues (see ³⁰ for more details).

192 2.2. Regulating services

193 Four regulating services were quantified per 3 m × 3 m plot, i.e., topsoil carbon storage, understorey
194 pollination potential, heatwave buffering and litter decomposition. The soil carbon stock (Mg/ha) in the
195 combined litter layer and mineral topsoil (0-20 cm) of each plot was used as a measure of the potential
196 topsoil carbon storage (see ³⁴). Pollination was assessed by the abundance-weighted average nectar
197 production potential of the understorey plant community per plot. Potential nectar production was
198 extracted per species from ³⁵ as the average of their upper and lower class limits. The latter are defined
199 in ³⁵ using a seven-degree logarithmic scale: 1 = no nectar production (0 g sugar m⁻² year⁻¹) and no
200 collectable pollen; 2 = nectar production insignificant (<0.2 g), or absent but with low but significant
201 amounts of collectable pollen; 3 = nectar production small (0.2–5 g), or lower but with copious
202 collectable pollen; 4 = nectar production modest (5–20 g); 5 = rather large (20–50 g); 6 = large (50–200
203 g); and 7 = very large (>200 g) (**Table S2**). The maximum summer temperature offset was used as a
204 proxy for the heatwave buffering (or 'cooling') capacity of the forest stands. Forest understorey
205 microclimates are generally buffered against severe temperature extremes³⁶, and this buffering effect,

206 and its effects on forest biodiversity and functioning, is most pronounced during summer³⁷.
207 Microclimate temperature was recorded hourly at 1 m above the soil surface in each vegetation plot
208 using miniature data loggers covered by radiation shields (type: Lascar EL-USB-1, range: -30 to 80 °C,
209 resolution: 0.5 °C). Temperature offsets were calculated for each plot by subtracting sub-canopy
210 temperatures (plot sensor) with temperature measured in open field close to each corresponding forest
211 stand (reference sensor). Positive (negative) offset values thus denote warmer (cooler) sub-canopy
212 temperatures compared to macroclimate temperatures. Maximum summer temperature offsets were
213 computed per plot as mean daily 95th percentile temperature during the summer months (April to
214 September 2019) (see ⁴). Finally, to quantify the decomposability of understorey leaf litter we used the
215 cover-weighted mean foliar C:N ratio of the five most abundant plant species in each plot as a proxy.
216 Leaf traits and especially foliar-level stoichiometry are a good indicator of ecosystem elemental cycling
217 and potential decomposition rates^{38,39}. Understorey decomposability can strongly influence nutrient
218 cycling rates in temperate forests as nutrient concentrations are on average 1.5 to 5 times higher in the
219 herbaceous understorey compared to the canopy tree foliage, depending on the nutrient considered (see
220 ⁴⁰ for a discussion). Besides, understorey leaf litter is generally more easily decomposable than tree leaf
221 litter, and provides a continuous input throughout the year as opposed to tree litter⁴¹. On top of that,
222 spring ephemerals play a particularly important role in nutrient circulation as they capture significant
223 amounts of nutrients from the soil in early spring when trees are still dormant, thereby preventing
224 leakage (often referred to as the “vernal dam hypothesis”⁴²).

225 2.3. Provisioning services

226 Three key provisioning services were calculated, i.e., timberwood, abundance of usable plants and tree
227 regeneration. Timberwood was quantified by the aboveground stem biomass in circular plots with 9 m
228 radius, which was determined per plot using multi-species biomass equations based on diameter at
229 breast height (DBH) developed by ⁴³. This generic equation was used because species-specific or local
230 allometric equations were not always available in the literature, and because the tree species pool was
231 especially large in this dataset (i.e. more than 40 different tree species across each of nine geographical
232 regions). Moreover, a validation by ³⁴ using only the Belgian plots in this dataset showed that local and

233 species-specific equations produced highly comparable biomass estimations ($R^2 = 0.98$). First, the DBH
234 of all standing trees within 9-m radius of each plot center was measured with a caliper. Two
235 perpendicular measurements per stem were performed and averaged. For multi-stemmed trees, all
236 individual stems (with $DBH \geq 7.5$ cm) were measured and treated as separate trees in the calculations.
237 Next, all tree species were classified by expert knowledge into the ten multi-species biomass groups
238 *sensu*⁴³. Each group represents a unique allometric equation based on DBH. As a final step, the stem
239 biomass estimations of all trees per plot were summed and converted to Mg per ha (see³⁴ for more
240 details). Note that the use of larger plots (necessary to accurately quantify this service)
241 unavoidably resulted in spatial autocorrelation between the plots close to the forest edge: with centers
242 of these plots at 1.5, 4.5 and 12.5 m from the edge, the circular 9-m plots partially overlapped. However,
243 an additional analysis showed that the effect of distance to the forest edge on stemwood biomass was
244 still significantly negative ($\beta = -0.154 \pm 0.059$, 95% CI = [-0.252, -0.060]) after excluding the data from
245 the plot at 4.5 m from the edge, thereby eliminating any overlap between plots. The abundance of usable
246 plants was assessed per 3 m x 3 m plot based on the vegetation composition. The potential use for food,
247 medical purposes or other uses of each plant species was determined based on different bibliographical
248 sources (**Table S2**), and their abundances were summed to obtain a total value per plot. Plants were
249 only considered 'usable' when used in Europe. Tree regeneration was assessed per 3 m x 3 m plot
250 during the time of the floristic surveys (May-June 2018) as the total abundance of tree seedlings across
251 all tree species in the understorey community of each plot.

252 3. Environmental predictor variables

253 3.1. Edaphic conditions

254 In each plot, five random subsamples of mineral topsoil were taken at 0-10 cm and 10-20 cm depth (30
255 mm diameter), and subsequently pooled per depth horizon. Samples were dried to constant weight at
256 40 °C for 48 h, ground and sieved over a 2 mm mesh. Then, they were analyzed for pH-H₂O by shaking
257 a 1:5 ratio soil/H₂O mixture for 5 min at 300 r.p.m. and measuring with an Orion 920A pH meter with
258 a Ross sure-flow 8172 BNWP pH electrode model (Thermo Scientific Orion, USA).

259 The same sampling procedure was followed for the soil samples taken between 10-20 cm depth for
260 texture analysis (% sand, silt and clay), which was performed by sieving and sedimentation with a
261 Robinson-Köhn pipette according to ISO 11277 (2009). The sand fraction was negatively correlated to
262 both the percentage of silt ($r = -0.81$; $p < 0.001$) and clay ($r = -0.80$; $p < 0.001$) in the soils. Silt and clay
263 fractions did not show a strong correlation with each other, but for the majority of the plots, the clay
264 fraction was rather low (<30%). Therefore, the sand fraction was used for further analysis as a proxy
265 for soil texture.

266 The organic soil horizon (litter, humus and fragmentation layer) was sampled in a 20 cm × 20 cm subplot
267 from its surface to the mineral soil horizon underneath, after removal of the herb layer. These samples
268 were subsequently dried to constant weight at 65 °C for 48h to determine the total mass of the organic
269 forest floor. This variable gives an indication of the quality and thickness in the litter layer as well as
270 nutrient availability because low-quality litter tends to degrade slowly and accumulates at the forest
271 floor resulting in slower nutrient turnover and lower nutrient availability. Moreover, thick litter layers
272 (e.g., in beech forests) may strongly impede emergence of tree saplings or forest herbs, while
273 germination can also be hampered through phytotoxic components⁴⁴. The variation of the three edaphic
274 conditions along the edge-to-interior gradient is shown in **Figure S1**.

275 3.2. Stand conditions

276 Plant area index (PAI) was used as a proxy for forest structure. It is defined as half of the surface area
277 of all aboveground plant parts (stems, branches and leaves) per unit surface area. Here PAI was
278 computed per plot as the integral of the vertically resolved plant area per volume density profiles (in
279 m^2/m^3). The latter were obtained from single-scan position terrestrial laser scanning (TLS) stationed in
280 the center of each plot using a RIEGL VZ-400 (RIEGL Laser Measurement Systems GmbH, Horn,
281 Austria), described in more detail in ³⁰. The PAI can be used as an indicator for forest structural
282 complexity and denseness of the canopy layer, and is thus negatively correlated to light availability at
283 the forest floor.

284 To characterize the composition of the overstorey (tree and shrub canopy), the average shade-casting
285 ability (SCA) was used. This variable was calculated per plot as the cover-weighted average of species-
286 specific SCA indices⁴⁵. These indices range from 1 (very low SCA, e.g. *Betula pubescens*) to 5 (high
287 ability of mature trees to cast shade, e.g. *Fagus sylvatica*), and are listed for all canopy species in ³⁰.

288 To quantify the microclimate in each plot, the air temperature was recorded at 1 m above the forest floor
289 using miniature temperature sensors (see Section 2.2). For each sensor, the absolute maximum
290 temperature of the warmest month (microclimate alternative for BIO5 in WorldClim⁴⁶) was calculated
291 as mean daily 95th percentile of maximum temperatures recorded underneath the canopy during the
292 warmest month of the measuring period. Such local temperature extremes are disproportionately
293 important for the response of organisms to climate warming since a species' relative fitness is strongly
294 determined by its heat tolerance⁴⁷. We use microclimate data instead of weather station data (free-air
295 temperature or macroclimate) as this provides more ecologically relevant information for forest
296 understories³⁶. The variation of the three forest stand conditions along the edge-to-interior gradient is
297 shown in **Figure S1**.

298 3.3. Landscape conditions

299 The amount of forest habitat in the landscape surrounding each forest stand was characterized by the
300 percentage area with a tree cover >20 % within a 500-m buffer zone. This variable was calculated based
301 on GIS analyses using a satellite-based global tree cover map with spatial resolution of 30 m developed
302 by ⁴⁸.

303 For each forest stand, drought was characterized by means of the Standardized Precipitation
304 Evapotranspiration Index (SPEI). The SPEI is a multi-scalar drought index based on macroclimatic
305 data, and can be used to identify the onset, duration and severity of drought conditions based on the
306 precipitation deficit and evaporative demand. The SPEI was calculated using the SPEI-package in R⁴⁹.
307 First, gridded monthly precipitation and evapotranspiration data were extracted from CRU TS v4
308 climate datasets⁵⁰ for the period 1901-2019. This data was used to calculate the monthly climatic water
309 balance (precipitation – evapotranspiration) for each site. Based on this water balance, monthly SPEI

310 values can be computed at time scales between 1 and 24 months prior to the survey (i.e. accounting for
311 the water balance of the previous 1 to 24 months). In this study, we specifically focused on the SPEI
312 index of May 2018 (onset of the data collection) accounting for the water balance of the previous 21
313 months (SPEI_{21-May2018}) because this value has been shown to exhibit the strongest correlation with
314 European forest health (i.e. crown defoliation⁵¹). Drought-induced defoliation of the tree canopy is
315 predicted to have important consequences for forest ecosystem functioning, e.g., by reducing
316 productivity and carbon sequestration but at the same time also stimulating tree regeneration^{52,53}.
317 Positive values of SPEI indicate a wet period, while negative values represent dry conditions relative to
318 the reference period of 1980-2015. Note that SPEI values ranging between -0.67 and 0.67 are considered
319 normal, while drought and severe drought are characterized by SPEI values below -0.67 and -1.28,
320 respectively⁵⁴.

321 Atmospheric pollution via nitrogen (N) deposition was estimated using modeled atmospheric N
322 deposition data from the European Monitoring and Evaluation Program (EMEP). Data was extracted
323 for the year 2016 at a resolution of 50 km × 50 km. For each forest stand, the total atmospheric N
324 deposition rate was calculated by summing the modeled rates of wet and dry oxidized and reduced N.
325 To account for higher N deposition rates in forest edges, values were corrected using a decreasing
326 exponential curve developed by⁵⁵. This curve was fitted based on in-situ throughfall measurements of
327 oxidized and reduced N in oak-dominated forest edges (see²⁹ for more details).

328 4. Statistical analysis

329 All models were fitted with the probabilistic programming language Stan using the *brms* package in R
330 version 4.2.1⁵⁶, and can be fully reproduced from an online repository:
331 <https://doi.org/10.6084/m9.figshare.22354069>. All biodiversity and ecosystem service indices were
332 normalized to have zero mean and unit variance (Z-scores) prior to analyses (**Table S3**). Normalization
333 puts indices on the same scale and enables efficient model estimation. To correct for skewness in some
334 of the scaled indices, an additional log-transformation was performed (see **Methods S1** for details). Due
335 to the hierarchical nature of the dataset, all models were fit with transect ID (levels corresponding to

336 the 45 edge-to-interior transects) nested within region (levels corresponding to nine regions) as random
337 intercepts to account for potential interdependence of plots located in the same transect or region.

338 A multivariate Bayesian model^{57,58} was fit to the four Z-transformed biodiversity indices and seven Z-
339 transformed ecosystem services as response variables to account for correlations among them (and thus
340 for potential trade-offs and synergies). A Gaussian error distribution was assumed allowing us to
341 estimate residual correlations in *brms*. In the first model, distance to the forest edge was included as
342 fixed effect. We used default priors (half-Student t with three degrees of freedom) which are weakly
343 informative, thereby having only minimal effect on the parameter estimates whilst improving sampling
344 efficiency and model convergence. The model was run with four independent chains of 4000 iterations
345 each after a warm-up of 2000 iterations in the Hamiltonian Markov Monte Carlo (HMC) and its
346 extension, the No-U-Turn sampler. The maximum tree depth was set to 12 and the target average
347 acceptance probability to 0.99 to allow proper sampling. For some biodiversity (taxonomic richness and
348 phylogenetic diversity) and ecosystem service (nectar production) indices, we assessed whether
349 including overstorey (shrub and tree) species influenced the observed distance to edge patterns.
350 However, the findings were virtually similar to those with only understorey species underpinning the
351 robustness of our analyses (see supplementary analysis in **Figure S2**).

352 In the second model, distance to the forest edge was substituted by a set of environmental variables as
353 fixed effects in the multivariate model. To represent edaphic conditions in each plot, sand fraction as a
354 proxy for soil texture, pH and organic layer mass as proxy for litter quality was used. For forest structure
355 and canopy composition, PAI, SCA and maximum microclimate temperature of warmest month was
356 included. To characterize landscape conditions, the percentage forest cover, SPEI (drought) index and
357 N deposition were used. The organic layer mass and N deposition were log-transformed due to their
358 skewed distribution. No interaction terms between environmental predictors were considered to reduce
359 complexity and avoid overparameterization of the model. Prior to running the model, multicollinearity
360 among the nine predictor variables was assessed using variance inflation factors (VIFs) through the *vif*
361 function in the *car* package⁵⁹. For all models, VIFs were smaller than 2, indicating that no
362 multicollinearity issues could be detected among the set of predictor variables (see ⁶⁰). All predictors

363 were standardized to zero mean and unit variance (Z-scores), as is recommended practice when working
364 with predictors on different scales. We used the same random effects, priors, warm-up, sampling and
365 model settings as in the first model described above.

366 Convergence and mixing of chains in the two models were visually inspected using the *bayesplot*
367 package⁶¹ as well as the Gelman-Rubin convergence statistic (Rhat)⁶². With $Rhat < 1.01$, the
368 convergence of all parameters was considered acceptable and sufficient samples were available for all
369 of them (i.e., the ratio of effective samples over the total number of post warm-up iterations was larger
370 than 10 %). Graphs show posterior means as well as two-sided 80 and 95 % Bayesian credible intervals
371 (CI) for all fixed model parameters. We considered modelled parameter estimates to demonstrate an
372 effect on the response variables if the Bayesian 95 % CIs of the posterior distribution did not overlap
373 with zero, and a marginal effect as the 80 % CIs did not overlap with zero. Model fits were evaluated
374 with posterior predictive checks (**Figure S3-S5**) as well as marginal and conditional R^2 using the
375 *bayes_R2* function in brms (**Table S4-S7**). A detailed description of the models is given in **Methods S1**.
376 In a final analysis, we quantified a multiservice delivery index for each plot and assessed how this index
377 varied along the edge-to-interior transects. This analysis revealed that there was no pattern in
378 multiservice delivery from edge to core in the forest patches, confirming the trade-offs we report in this
379 study (with the supply potential of some services being greater in the edge and others greater in the
380 interior, hence masking a pattern in multiservice delivery). Details and results of this analysis are given
381 in **Extended Data Figure 3, Figure S6 and Table S8-S9**.

382 **Data Availability**

383 All data needed to reproduce the analyses and figures presented in this study are available on Figshare
384 (<https://doi.org/10.6084/m9.figshare.24559891.v1>) and GitHub ([https://github.com/to-](https://github.com/to-vanneste/tradeoffs.git)
385 [vanneste/tradeoffs.git](https://github.com/to-vanneste/tradeoffs.git)).

386 **Code Availability**

387 All R code needed to reproduce the analyses and figures presented in this study are available on Figshare
388 (<https://doi.org/10.6084/m9.figshare.24559891.v1>) and GitHub ([https://github.com/to-
vanneste/tradeoffs.git](https://github.com/to-
389 vanneste/tradeoffs.git)).

390 **Acknowledgements**

391 Special thanks go to Luc Willems and Greet De Bruyn for performing the chemical analysis and to
392 Abdulwahhab Ghairi for the texture analysis. We also thank Evy Ampoorter, Haben Blondeel, Filip
393 Ceunen, Kris Ceunen, Robbe De Beelde, Emiel De Lombaerde, Kent Hansson, Lionel Hertzog, Dries
394 Landuyt, Pierre Lhoir, Sruthi M. Krishna Moorthy, Audrey Peiffer, Michael Perring, Matteo Tolosano,
395 Sanne Van Den Berge, Lotte Van Nevel and Mia Vedel-Sørensen for their assistance during the
396 fieldwork. TV, LD, EDL, CM, PS, PVG and PDF received funding through the ERC Starting grant
397 FORMICA (no. 757833, <http://www.formica.ugent.be>). SG, KDP and LD were supported by the
398 Research Foundation Flanders (FWO) (no. G0H1517N, ASP035-19, and 1221523N respectively). The
399 plot network and data collection were realized through the FWO Scientific research network FLEUR
400 (<http://www.fleur.ugent.be>).

401 **Author Contributions Statement**

402 TV, LD, PDF, PV and KV conceived and designed the study. EDL, CM, SG, KDP, PS, KB, JB, KC,
403 SAOC, MD, CG, BJG, P-OH, GI, JL, SL, AO, QP, JP, FS, FS, HV, FZ and PV collected the data. CM,
404 SG, KDP and PS processed the data, while TV and LD performed the data analyses under supervision
405 of PDF and KV. TV and LD drafted the manuscript and all authors contributed to later versions.

406 **Competing Interests Statement**

407 The authors declare no competing interests.

408 **Tables**

409 /

410 **Figure legends/captions**

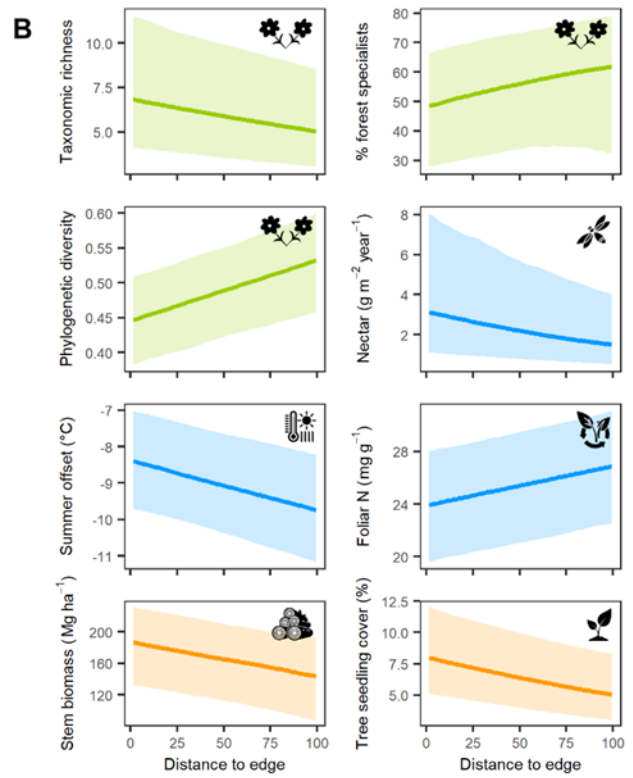
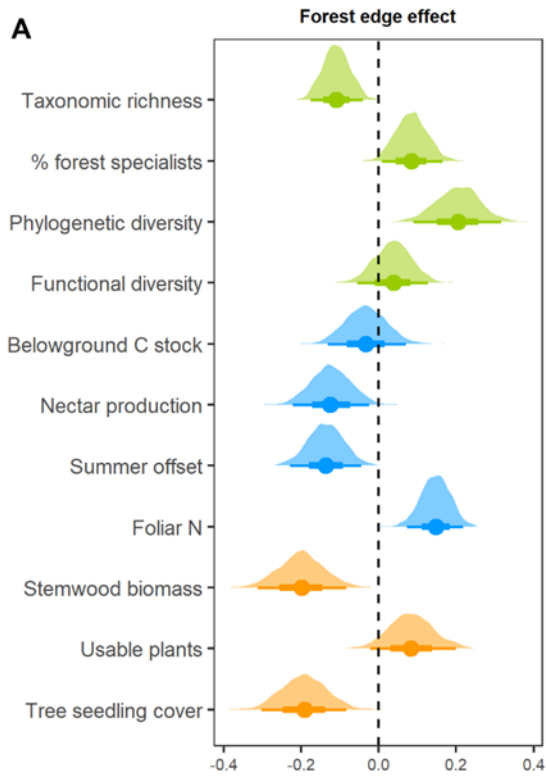
411 **Figure 1. Effect of distance to the forest edge on biodiversity and ecosystem service indices.**

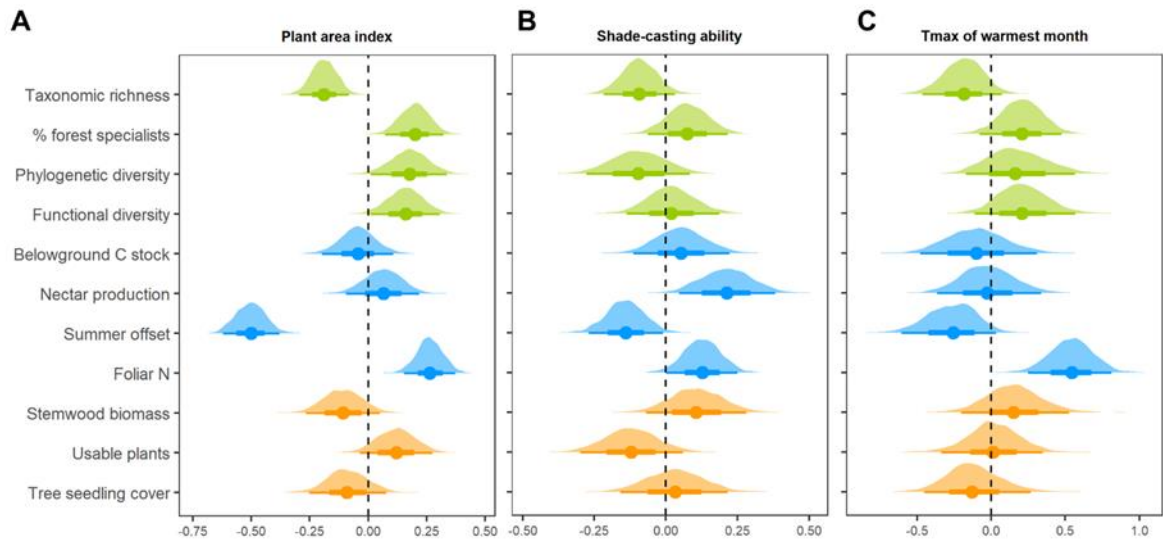
412 (A) Distance to edge effects on the considered biodiversity and ecosystem service indices quantified
413 for each 3 m × 3 m plot in the forest-edge-to-interior transects (n = 225 biologically independent plots).
414 Circles represent mean standardized effect sizes with 80% (thick line) and 95% credible intervals (thin
415 line) and distributions obtained from a multivariate Bayesian model. (B) Edge-to-interior gradients of
416 biodiversity and ecosystem service indices for which 95% credible intervals don't overlap zero. All
417 datapoints are shown as circles and represent the 3 m × 3 m plots (n = 225) in the forest-edge-to-interior
418 transects. Lines and shading denote mean model predictions ± 95% credible intervals from Bayesian
419 models. Colours denote biodiversity indices (green), regulating (blue) and provisioning ecosystem
420 services (orange). The selected biodiversity indices are taxonomic richness, proportion of forest
421 specialists, phylogenetic diversity and functional trait diversity of the forest understorey plant
422 communities, while the ecosystem service indicators are soil carbon storage (as proxy for soil C
423 sequestration), nectar production (as proxy for pollination potential), summer offset (as proxy for
424 heatwave buffering capacity), foliar C:N ratio (as proxy for litter decomposition), stemwood biomass
425 (as proxy for timberwood), abundance of usable plants and tree seedling cover (as proxy for
426 regeneration). Given that the response variables were normalised using Z-scores in the multivariate
427 model, a back-transformation was used in the different subpanels for a clearer visual interpretation.
428 Icons were extracted from The Noun Project (<https://thenounproject.com>).

429 **Figure 2. Effect of forest stand characteristics on biodiversity and ecosystem service indices.**

430 Effect of plant area index (A), shade-casting ability (B) and maximum understorey (microclimate)
431 temperature of the warmest month (C) on the biodiversity and ecosystem service indices quantified for
432 each 3 m × 3 m plot in the forest-edge-to-interior transects (n = 225 biologically independent plots).
433 Circles represent mean standardized effect sizes with 80% (thick line) and 95 % credible intervals (thin
434 line) and distributions obtained from a multivariate Bayesian model. Colours denote biodiversity
435 indices (green), regulating (blue) and provisioning ecosystem services (orange). The selected

436 biodiversity indices are taxonomic richness, proportion of forest specialists, phylogenetic diversity and
437 functional trait diversity of the forest understorey plant communities, while the ecosystem service
438 indicators are soil carbon storage (as proxy for soil C sequestration), nectar production (as proxy for
439 pollination potential), summer offset (as proxy for heatwave buffering capacity), foliar C:N ratio (as
440 proxy for litter decomposition), stemwood biomass (as proxy for timberwood), abundance of usable
441 plants and tree seedling cover (as proxy for regeneration). Effects of the other environmental drivers
442 (edaphic and landscape conditions) are shown in **Extended Data Figure 4**.





447

448 **References**

449 1 FAO (2015). Global Forest Resource Assessment 2015. FAO, Rome: 105 pp.

450 2 Valdés, A., Lenoir, J., De Frenne, P., Andrieu, E., Brunet, J., Chabrierie, O., ... & Decocq, G. (2020).
451 High ecosystem service delivery potential of small woodlands in agricultural landscapes. *Journal of*
452 *Applied Ecology*, 57(1), 4-16.

453 3 Hertzog, L. R., Boonyarittichaikij, R., Dekeukeleire, D., de Groot, S. R., van Schroyen Lantman,
454 I. M., Sercu, B. K., ... & Baeten, L. (2019). Forest fragmentation modulates effects of tree species
455 richness and composition on ecosystem multifunctionality. *Ecology*, 100(4), e02653.

456 4 Meeussen, C., Govaert, S., Vanneste, T., Bollmann, K., Brunet, J., Calders, K., ... & De Frenne, P.
457 (2021). Microclimatic edge-to-interior gradients of European deciduous forests. *Agricultural and Forest*
458 *Meteorology*, 311, 108699.

459 5 Schmidt, M., Jochheim, H., Kersebaum, K. C., Lischeid, G., & Nendel, C. (2017). Gradients of
460 microclimate, carbon and nitrogen in transition zones of fragmented landscapes – a review. *Agricultural*
461 *and Forest Meteorology*, 232, 659-671.

462 6 Remy, E., Wuyts, K., Boeckx, P., Gundersen, P., & Verheyen, K. (2017). Edge effects in temperate
463 forests subjected to high nitrogen deposition. *Proceedings of the National Academy of Sciences*,
464 114(34), E7032-E7032.

465 7 Pfeifer, M., Lefebvre, V., Peres, C. A., Banks-Leite, C., Wearn, O. R., Marsh, C. J., ... & Ewers, R.
466 M. (2017). Creation of forest edges has a global impact on forest vertebrates. *Nature*, 551(7679), 187-
467 191.

468 8 Taubert, F., Fischer, R., Groeneveld, J., Lehmann, S., Müller, M. S., Rödiger, E., ... & Huth, A. (2018).
469 Global patterns of tropical forest fragmentation. *Nature*, 554(7693), 519-522.

- 470 **9** Haddad, N. M., Brudvig, L. A., Clobert, J., Davies, K. F., Gonzalez, A., Holt, R. D., ... & Townshend,
471 J. R. (2015). Habitat fragmentation and its lasting impact on Earth's ecosystems. *Science advances*,
472 1(2), e1500052.
- 473 **10** Riitters, K., Wickham, J., Costanza, J. K., & Vogt, P. (2016). A global evaluation of forest interior
474 area dynamics using tree cover data from 2000 to 2012. *Landscape Ecology*, 31(1), 137-148.
- 475 **11** Estreguil, C., Caudullo, G., de Rigo, D., & San-Miguel-Ayanz, J. (2013). Forest landscape in Europe:
476 pattern, fragmentation and connectivity. *EUR Scientific and Technical Research*, 25717.
- 477 **12** Shapiro, A. C., Aguilar-Amuchastegui, N., Hostert, P., & Bastin, J. F. (2016). Using fragmentation
478 to assess degradation of forest edges in Democratic Republic of Congo. *Carbon balance and*
479 *management*, 11(1), 1-15.
- 480 **13** Landuyt, D., De Lombaerde, E., Perring, M. P., Hertzog, L. R., Ampoorter, E., Maes, S. L., ... &
481 Verheyen, K. (2019). The functional role of temperate forest understorey vegetation in a changing
482 world. *Global Change Biology*, 25(11), 3625-3641.
- 483 **14** Thrippleton, T., Bugmann, H., Folini, M., & Snell, R. S. (2018). Overstorey–understorey interactions
484 intensify after drought-induced forest die-off: long-term effects for forest structure and composition.
485 *Ecosystems*, 21(4), 723-739.
- 486 **15** Chastain Jr, R. A., Currie, W. S., & Townsend, P. A. (2006). Carbon sequestration and nutrient
487 cycling implications of the evergreen understory layer in Appalachian forests. *Forest Ecology and*
488 *Management*, 231(1-3), 63-77.
- 489 **16** De Lombaerde, E., Baeten, L., Verheyen, K., Perring, M. P., Ma, S., & Landuyt, D. (2021).
490 Understorey removal effects on tree regeneration in temperate forests: A meta-analysis. *Journal of*
491 *Applied Ecology*, 58(1), 9-20.

492 **17** Perring, M. P., Diekmann, M., Midolo, G., Costa, D. S., Bernhardt-Römermann, M., Otto, J. C., ...
493 & Verheyen, K. (2018). Understanding context dependency in the response of forest understorey plant
494 communities to nitrogen deposition. *Environmental pollution*, 242, 1787-1799.

495 **18** Zellweger, F., De Frenne, P., Lenoir, J., Vangansbeke, P., Verheyen, K., Bernhardt-Römermann,
496 M., ... & Coomes, D. (2020). Forest microclimate dynamics drive plant responses to warming. *Science*,
497 368(6492), 772-775.

498 **19** Le Bagousse-Pinguet, Y., Soliveres, S., Gross, N., Torices, R., Berdugo, M., & Maestre, F. T. (2019).
499 Phylogenetic, functional, and taxonomic richness have both positive and negative effects on ecosystem
500 multifunctionality. *Proceedings of the National Academy of Sciences*, 116(17), 8419-8424.

501 **20** Van der Plas, F., Manning, P., Allan, E., Scherer-Lorenzen, M., Verheyen, K., Wirth, C., ... &
502 Fischer, M. (2016). Jack-of-all-trades effects drive biodiversity–ecosystem multifunctionality
503 relationships in European forests. *Nature communications*, 7(1), 1-11.

504 **21** Calders, K., Newnham, G., Burt, A., Murphy, S., Raunonen, P., Herold, M., ... & Kaasalainen, M.
505 (2015). Nondestructive estimates of above-ground biomass using terrestrial laser scanning. *Methods in*
506 *Ecology and Evolution*, 6(2), 198-208.

507 **22** Thompson, P. L., & Gonzalez, A. (2016). Ecosystem multifunctionality in metacommunities.
508 *Ecology*, 97(10), 2867-2879.

509 **23** Gough, C. M., Atkins, J. W., Fahey, R. T., & Hardiman, B. S. (2019). High rates of primary
510 production in structurally complex forests. *Ecology* 100(10), e02864

511 **24** Penone, C., Allan, E., Soliveres, S., Felipe-Lucia, M. R., Gossner, M. M., Seibold, S., ... & Fischer,
512 M. (2019). Specialisation and diversity of multiple trophic groups are promoted by different forest
513 features. *Ecology letters*, 22(1), 170-180.

514 **25** Ehbrecht, M., Seidel, D., Annighöfer, P., Kreft, H., Köhler, M., Zemp, D. C., ... & Ammer, C. (2021).
515 Global patterns and climatic controls of forest structural complexity. *Nature communications*, 12(1), 1-
516 12.

517 **26** Karger, D. N., Nobis, M. P., Normand, S., Graham, C. H., & Zimmermann, N. E. (2021). CHELSA-
518 TraCE21k v1. 0. Downscaled transient temperature and precipitation data since the last glacial
519 maximum. *Climate of the Past Discussions*, 1-27

520 **27** Brus, D. J., Hengeveld, G. M., Walvoort, D. J. J., Goedhart, P. W., Heidema, A. H., Nabuurs, G. J.,
521 & Gunia, K. (2012). Statistical mapping of tree species over Europe. *European Journal of Forest*
522 *Research*, 131(1), 145-157.

523 **28** Govaert, S., Meeussen, C., Vanneste, T., Bollmann, K., Brunet, J., Cousins, S. A., ... & De Frenne,
524 P. (2020). Edge influence on understorey plant communities depends on forest management. *Journal of*
525 *Vegetation Science*, 31(2), 281-292.

526 **29** Meeussen, C., Govaert, S., Vanneste, T., Calders, K., Bollmann, K., Brunet, J., ... & De Frenne, P.
527 (2020). Structural variation of forest edges across Europe. *Forest Ecology and Management*, 462,
528 117929.

529 **30** De Pauw, K., Meeussen, C., Govaert, S., Sanczuk, P., Vanneste, T., Bernhardt-Römermann, M., ...
530 & De Frenne, P. (2021). Taxonomic, phylogenetic and functional diversity of understorey plants
531 respond differently to environmental conditions in European forest edges. *Journal of Ecology*, 109(7),
532 2629-2648.

533 **31** Heinken, T., Diekmann, M., Liira, J., Orczewska, A., Schmidt, M., Brunet, J., ... & Vanneste, T.
534 (2022). The European Forest Plant Species List (EuForPlant): Concept and applications. *Journal of*
535 *Vegetation Science*, 33(3), e13132.

536 **32** Zanne, A. E., Tank, D. C., Cornwell, W. K., Eastman, J. M., Smith, S. A., FitzJohn, R. G., ... &
537 Beaulieu, J. M. (2014). Three keys to the radiation of angiosperms into freezing environments. *Nature*,
538 506(7486), 89-92.

539 **33** Laliberté, E., & Legendre, P. (2010). A distance-based framework for measuring functional diversity
540 from multiple traits. *Ecology*, 91(1), 299-305.

541 **34** Meeussen, C., Govaert, S., Vanneste, T., Haesen, S., Van Meerbeek, K., Bollmann, K., ... & De
542 Frenne, P. (2021). Drivers of carbon stocks in forest edges across Europe. *Science of the Total*
543 *Environment*, 759, 143497.

544 **35** Tyler, T., Herbertsson, L., Olofsson, J., & Olsson, P. A. (2021). Ecological indicator and traits values
545 for Swedish vascular plants. *Ecological Indicators*, 120, 106923.

546 **36** De Frenne, P., Zellweger, F., Rodríguez-Sánchez, F., Scheffers, B. R., Hylander, K., Luoto, M., ...
547 & Lenoir, J. (2019). Global buffering of temperatures under forest canopies. *Nature Ecology &*
548 *Evolution*, 3(5), 744-749.

549 **37** Zellweger, F., Coomes, D., Lenoir, J., Depauw, L., Maes, S. L., Wulf, M., ... & De Frenne, P. (2019).
550 Seasonal drivers of understorey temperature buffering in temperate deciduous forests across Europe.
551 *Global Ecology and Biogeography*, 28(12), 1774-1786.

552 **38** Xu, S., Sardans, J., Zhang, J., & Peñuelas, J. (2020). Variations in foliar carbon: nitrogen and
553 nitrogen: phosphorus ratios under global change: A meta-analysis of experimental field studies.
554 *Scientific reports*, 10(1), 12156.

555 **39** Chen, X., & Chen, H. Y. (2021). Plant mixture balances terrestrial ecosystem C: N: P stoichiometry.
556 *Nature Communications*, 12(1), 4562.

557 **40** Landuyt, D., De Lombaerde, E., Perring, M. P., Hertzog, L. R., Ampoorter, E., Maes, S. L., ... &
558 Verheyen, K. (2019). The functional role of temperate forest understorey vegetation in a changing
559 world. *Global Change Biology*, 25(11), 3625-3641.

560 **41** Muller, R. N. (2003). Deciduous Forest Ecosystems. The herbaceous layer in forests of eastern North
561 America, 15.

562 **42** Mabry, C. M., Gerken, M. E., & Thompson, J. R. (2008). Seasonal storage of nutrients by perennial
563 herbaceous species in undisturbed and disturbed deciduous hardwood forests. *Applied Vegetation*
564 *Science*, 11(1), 37-44.

565 **43** Jenkins, J. C., Chojnacky, D. C., Heath, L. S., & Birdsey, R. A. (2003). National-scale biomass
566 estimators for United States tree species. *Forest science*, 49(1), 12-35.

567 **44** Dzwonko, Z., & Gawroński, S. (2002). Effect of litter removal on species richness and acidification
568 of a mixed oak-pine woodland. *Biological Conservation*, 106(3), 389-398.

569 **45** Verheyen, K., Baeten, L., De Frenne, P., Bernhardt-Römermann, M., Brunet, J., Cornelis, J., ... &
570 Verstraeten, G. (2012). Driving factors behind the eutrophication signal in understorey plant
571 communities of deciduous temperate forests. *Journal of Ecology*, 100(2), 352-365.

572 **46** Fick, S. E., & Hijmans, R. J. (2017). WorldClim 2: new 1-km spatial resolution climate surfaces for
573 global land areas. *International journal of climatology*, 37(12), 4302-4315.

574 **47** Huey, R. B., Kearney, M. R., Krockenberger, A., Holtum, J. A., Jess, M., & Williams, S. E. (2012).
575 Predicting organismal vulnerability to climate warming: roles of behaviour, physiology and adaptation.
576 *Philosophical Transactions of the Royal Society B: Biological Sciences*, 367(1596), 1665-1679.

577 **48** Hansen, M. C., Potapov, P. V., Moore, R., Hancher, M., Turubanova, S. A., Tyukavina, A., ... &
578 Townshend, J. (2013). High-resolution global maps of 21st-century forest cover change. *science*,
579 342(6160), 850-853.

580 **49** Santiago Beguería and Sergio M. Vicente-Serrano (2017). SPEI: Calculation of the Standardised
581 Precipitation-Evapotranspiration Index. R package version 1.7. [https://CRAN.R-](https://CRAN.R-project.org/package=SPEI)
582 [project.org/package=SPEI](https://CRAN.R-project.org/package=SPEI)

583 **50** Harris, I., Osborn, T. J., Jones, P., & Lister, D. (2020). Version 4 of the CRU TS monthly high-
584 resolution gridded multivariate climate dataset. *Scientific data*, 7(1), 1-18.

585 **51** Sousa-Silva, R., Verheyen, K., Ponette, Q., Bay, E., Sioen, G., Titeux, H., ... & Muys, B. (2018).
586 Tree diversity mitigates defoliation after a drought-induced tipping point. *Global Change Biology*,
587 24(9), 4304-4315.

588 **52** Grossiord, C., Granier, A., Ratcliffe, S., Bouriaud, O., Bruelheide, H., Chećko, E., ... & Gessler, A.
589 (2014). Tree diversity does not always improve resistance of forest ecosystems to drought. *Proceedings*
590 *of the National Academy of Sciences*, 111(41), 14812-14815.

591 **53** Guada, G., Camarero, J. J., Sánchez-Salguero, R., & Cerrillo, R. M. N. (2016). Limited growth
592 recovery after drought-induced forest dieback in very defoliated trees of two pine species. *Frontiers in*
593 *Plant Science*, 7, 418.

594 **54** Isbell, F., Calcagno, V., Hector, A., Connolly, J., Harpole, W. S., Reich, P. B., ... & Loreau, M.
595 (2011). High plant diversity is needed to maintain ecosystem services. *Nature*, 477(7363), 199-202.

596 **55** Wuyts, K., De Schrijver, A., Staelens, J., Gielis, L., Vandenbruwane, J., & Verheyen, K. (2008).
597 Comparison of forest edge effects on throughfall deposition in different forest types. *Environmental*
598 *Pollution*, 156(3), 854-861.

599 **56** R Core Team (2021). R: A language and environment for statistical computing. R Foundation for
600 Statistical Computing, Vienna, Austria. URL <https://www.R-project.org/>.

601 **57** Bürkner Paul-Christian (2017). brms: An R Package for Bayesian Multilevel Models Using Stan.
602 *Journal of Statistical Software*, 80(1), 1-28. doi:10.18637/jss.v080.i01

603 **58** Bürkner Paul-Christian (2021). Bayesian Item Response Modeling in R with brms and Stan. *Journal*
604 *of Statistical Software*, 100(5), 1-54. doi:10.18637/jss.v100.i05

- 605 **59** Fox John and Weisberg Sanford (2019). An R Companion to Applied Regression, Third Edition.
606 Thousand Oaks CA: Sage. URL: <https://socialsciences.mcmaster.ca/jfox/Books/Companion/>
- 607 **60** Zuur, A. F., Ieno, E. N., Walker, N. J., Saveliev, A. A., & Smith, G. M. (2009). Mixed effects models
608 and extensions in ecology with R (Vol. 574). New York: Springer.
- 609 **61** Gabry J, Mahr T (2021). “bayesplot: Plotting for Bayesian Models.” R package version 1.8.1,
610 URL: <https://mc-stan.org/bayesplot/>.
- 611 **62** Gelman, A., & Rubin, D. B. (1992). Inference from iterative simulation using multiple sequences.
612 Statistical science, 7(4), 457-472.
- 613 **63** Slade EM, Kirwan L, Bell T, Philipson CD, Lewis OT, Roslin T (2017) The importance of species
614 identity and interactions for multifunctionality depends on how ecosystem functions are valued.
615 Ecology 98:2626–2639